Molecular Medicine

Administration of α-Galactosylceramide Improves Adenine-Induced Renal Injury

Cristhiane Favero Aguiar,[1,2] Cristiane Naffah-de-Souza,[2] Angela Castoldi,[2] Matheus Corrêa-Costa,[2] Tárcio T Braga,[2] Érika L Naka,[1] Mariane T Amano,[2] Débora T R S Abate,[2] Meire I Hiyane,[2] Marcos A Cenedeze,[1] Alvaro Pacheco e Silva Filho,[1,3] and Niels O S Câmara[1,2]

[1]Laboratory of Clinical and Experimental Immunology, Nephrology Division, Federal University of São Paulo, São Paulo, Brazil; [2]Laboratory of Transplantation Immunobiology, Department of Immunology, Institute of Biomedical Sciences IV, University of São Paulo, São Paulo, Brazil; and [3]Instituto Israelita de Ensino e Pesquisa Albert Einstein, Renal Transplantation Unit, Albert Einstein Hospital, São Paulo, Brazil

Natural killer T (NKT) cells are a subset of lymphocytes that reacts to glycolipids presented by CD1d. Invariant NKT cells (iNKT) correspond to >90% of the total population of NKTs and reacts to α-galactosylceramide (αGalCer). αGalCer promotes a complex mixture of Th1 and Th2 cytokines, as interferon (IFN)-γ and interleukin (IL)-4. NKT cells and IFN-γ are known to participate in some models of renal diseases, but further studies are still necessary to elucidate their mechanisms. The aim of our study was to analyze the participation of iNKT cells in an experimental model of tubule-interstitial nephritis. We used 8-wk-old C57BL/6j, Jα18KO and IFN-γKO mice. They were fed a 0.25% adenine diet for 10 d. Both adenine-fed wild-type (WT) and Jα18KO mice exhibited renal dysfunction, but adenine-fed Jα18KO mice presented higher expression of kidney injury molecule-1 (KIM-1), tumor necrosis factor (TNF)-α and type I collagen. To analyze the role of activated iNKT cells in our model, we administered αGalCer in WT mice during adenine ingestion. After αGalCer injection, we observed a significant reduction in serum creatinine, proinflammatory cytokines and renal fibrosis. However, this improvement in renal function was not observed in IFN-γKO mice after αGalCer treatment and adenine feeding, illustrating that this cytokine plays a role in our model. Our findings may suggest that IFN-γ production is one of the factors contributing to improved renal function after αGalCer administration.

Online address: http://www.molmed.org
doi: 10.2119/molmed.2014.00090

INTRODUCTION

Chronic kidney diseases (CKDs) are progressive scarring conditions characterized by a decrease in renal function over time affecting millions of people worldwide. A common final pathway of CKD is tubule-interstitial fibrosis, caused by excessive extracellular matrix deposition after chronic insults (1,2).

Independently of which renal compartment is affected, an inflammatory process is usually present in kidney diseases, and such a process can be resumed in some steps. First, a physical or chemical injury (for example, hypertension, drugs and obstruction) may cause a release of inflammatory mediators, which recruit inflammatory cells to the site. Such an inflammatory process affects tubular cells and may lead to apoptosis, necrosis or activation of interstitial fibroblasts, which produce collagens leading to a fibrotic scar (3–5).

In 1985, Yokozawa *et al.* (6) demonstrated that an excessive intake of adenine would lead to renal injury. Adenine is produced endogenously but its long-term ingestion results in 2,8-dihydroxyadenine precipitation inside the renal tubules, leading to the formation of kidney stones, with extensive tubular dilation, inflammation, necrosis and fibrosis. The inflammatory process in this model is known to comprise the activation of toll-like receptors, inflammasome and nuclear factor (NF)-κB (2,7–9).

Furthermore, the involvement of immune cells is also a central step in the development of renal diseases. Various cell types infiltrate the kidney during the inflammatory process, for example, neutrophils, macrophages, T cells and others. A distinct subtype of T cells, called natural killer T (NKT) cells, might also be present in some kidney diseases.

NKT cells constitute a distinct population of lymphocytes found at low frequency (<1% in the peripheral blood of mice and humans) and characterized by

Address correspondence to *Niels O S Câmara, Institute of Biomedical Sciences IV, University of São Paulo, Av. Prof. Lineu Prestes, 1730, 05508-900, São Paulo, SP, Brazil. Phone: +55-11-30917388; Fax: +55-11-30917224; E-mail: niels@icb.usp.br.*
Submitted April 28, 2014; Accepted for publication June 12, 2015; Published Online (www.molmed.org) June 18, 2015.

their reactivity to glycolipids presented by CD1d, a molecule similar to MHC class I (10). Two major subtypes of NKT cells are currently recognized: type I and type II (11,12). Type I NKT cells, also called invariant NKT (iNKT), express a T-cell receptor (TCR) with a canonical rearrangement formed by a constant α chain (Vα14Jα18 in mice and Vα24Jα18 in humans) paired with a strict repertoire of β chains (Vβ8, Vβ7, Vβ2 in mice and Vβ11 in humans). iNKT cells correspond to >90% of the total population of NKT and react to the glycolipid α-galactosylceramide (αGalCer, also called KRN7000) and its analogs. αGalCer is a potent activator of both human and murine NKT cells and promotes a complex mixture of Th1 and Th2 cytokines, with an explosive release of interleukin (IL)-4 and large quantities of interferon (IFN)-γ (13–15).

IFN-γ is a potent cytokine with important and distinct functions. It is essential to host protection against intracellular pathogens but it can also contribute to autoimmunity (16). Thus, IFN-γ has different roles in inflammation and immune regulation depending on the conditions and influences from the microenvironment.

Since the role of NKT cell, and its cytokines (for example, IFN-γ), in renal diseases is still not fully elucidated, we aimed to analyze the involvement of these cells in an experimental model of tubule-interstitial nephritis.

MATERIALS AND METHODS

Animals

We used male C57BL/6J, Jα18KO and IFN-γKO mice, 8–10 wks old. The Jα18KO mice were a gift from Dr. Masaru Taniguchi at the RIKEN Research Center for Allergy and Immunology (Japan) (17). All mice were kept in well-controlled animal housing facilities and had free access to water and food. Animals were provided by the animal facility of the Center for Development of Experimental Models for Medicine and Biology (CEDEME-UNIFESP, São Paulo, Brazil). All animal experiments were performed according to the Ethics Committee of the Federal University of São Paulo (number 2010/1517).

Tubule-Interstitial Nephritis Induction

To induce tubule-interstitial nephritis (TIN), mice were fed a diet containing 0.25% adenine (Rhoster) *ad libitum* for 10 d (8). Control mice were fed the standard diet. Blood and kidney samples were collected for analysis at d 4 and 10. Serum creatinine was measured by Jaffé's modified method by using commercially purchased kits (Creatinine Kit, Labtest). Serum samples were deproteinizated before the colorimetric assay. NGAL (neutrophil gelatinase-associated lipocalin) (18) was measured in kidney tissue extract by using the commercially purchased kit Mouse NGAL ELISA Kit (BIOPORTO Diagnostics) according to the manufacturer's protocol. NGAL is a type 1 acute phase protein that is upregulated in mouse kidney cells after some virus infection and in postischemic and nephrotoxic
injury (19–21).

Another parameter used to assess TIN induction was kidney injury molecule-1 (*KIM-1*) mRNA expression. KIM-1 is a transmembrane protein that has been described to be highly expressed in the kidney after ischemia (22).

αGalCer Administration

C57BL/6J wild-type (WT) and IFN-γKO mice were injected intraperitoneally with 5 μg αGalCer in 200 μL phosphate-buffered saline (PBS) + 0.5% polysorbate-20. αGalCer is a potent activator of both murine and human iNKT cells and induces the production of a complex mixture of Th1 and Th2 cytokines (14). αGalCer was obtained from Alexis Biochemicals, and it was initially solubilized in chloroform:methanol (2:1) to make aliquots. Solvent was removed from the aliquots by drying in nitrogen atmosphere; for use, the glycolipid was then resuspended to PBS + 0.5% polysorbate-20 and sonicated for 90 min at 60°C.

Quantitative Real-Time Polymerase Chain Reaction

Total RNA was extracted from a kidney section by using TRIzol Reagent (Invitrogen). First-strand cDNAs were synthesized using the Moloney murine leukemia virus (M-MLV) reverse-transcriptase kit (Promega). Real-time polymerase chain reaction (PCR) was performed on a GeneAmp 7300 Sequence Detection System (Applied Biosystems) by using SYBR Green, TaqMan Gene expression assays (Applied Biosystems) and PrimeTime® qPCR primers (Integrated DNA Technologies). Messenger RNA expression for each signal was calculated by using the delta threshold cycle (ΔCt) procedure. Hypoxanthine-guanine phosphoribosyltransferase (*HPRT*) was used as a reference gene. The primer sets are summarized in Supplementary Tables S1 and S2. Samples were run in triplicate. The relative expression amounts of the target mRNA to *HPRT* were calculated with the following equations. Relative expression level of the target mRNA = $2^{-\Delta\Delta Ct}$.

Histological Analysis

Formalin-fixed, paraffin-embedded kidney sections were deparaffinized and stained with Sirius red for histological analysis. Renal tissues were then visualized under polarized light, and the percentage of cortex fibrosis was quantified by using the ImageJ software.

A histopathologist, unaware of the type of treatment, evaluated histological changes semiquantitatively. Twenty fields per kidney at 200× magnification were examined for tubular injury by using a semiquantitative scale (23). Scores were assigned according to the percentage of cortical tubules having alterations, as follows: 0.0%; 1, unchanged, <10%; 2, slight change, 10–25%; 3, moderate alteration, 26–75%; or 4, intense alteration, >75%.

Immunohistochemistry for Fibroblast-Specific Protein-1 (FSP-1) and α–Smooth Muscle Actin (α-SMA)

Renal interstitial fibrosis is also characterized by excessive deposition of extracellular matrix and accumulation of

fibroblasts (24). Although other cell types may be involved, the fibroblasts can be considered as key mediators of renal fibrosis (25,26). Given the important role of fibroblasts, we analyzed in our study the FSP-1 expression in renal tissue and also α-SMA, which is related to the contractile function acquired by the myofibroblasts during the fibrotic process.

Thin sections of the renal tissue were deparaffinized and dehydrated by a series of xylene and alcohol washes. For antigen retrieval, sections were microwaved (10 min) in Tris-EDTA (ethylenediaminetetraacetic acid) buffer. Endogenous peroxidase activity was blocked with 3% (v/v) H_2O_2 for 10 min. Tissues were incubated with Protein Block (DAKO) and then with monoclonal antibody S100A4 (1:500) for 4 h at room temperature or with α-SMA antibody (1:50) overnight. The slides with tissue sections were incubated with the polymer (Envision, DAKO) for 30 min. The reaction was stained with diaminobenzidine followed by hematoxylin counterstaining. The presence of FSP-1 and α-SMA in renal tissue was quantified as a percentage in the cortex using software for image analysis (NIS, Elements Advanced Research).

Cytometric Bead Array

Cytometric bead array for mouse cytokines (BD Biosciences) was performed to quantify IL-6 and tumor necrosis factor (TNF)-α in serum and kidney extracts, as described by the manufacturer.

Statistical Analysis

Results are expressed as mean ± standard deviation. One-way analysis of variance (ANOVA) and Tukey posttest were performed to compare groups using GraphPad Prism 5.0 (GraphPad Software). Reverse transcriptase PCR results are presented as a ratio of the calibrator gene *HPRT* and presented in arbitrary units. Differences were considered statistically significant when p was <0.05.

All supplementary materials are available online at www.molmed.org.

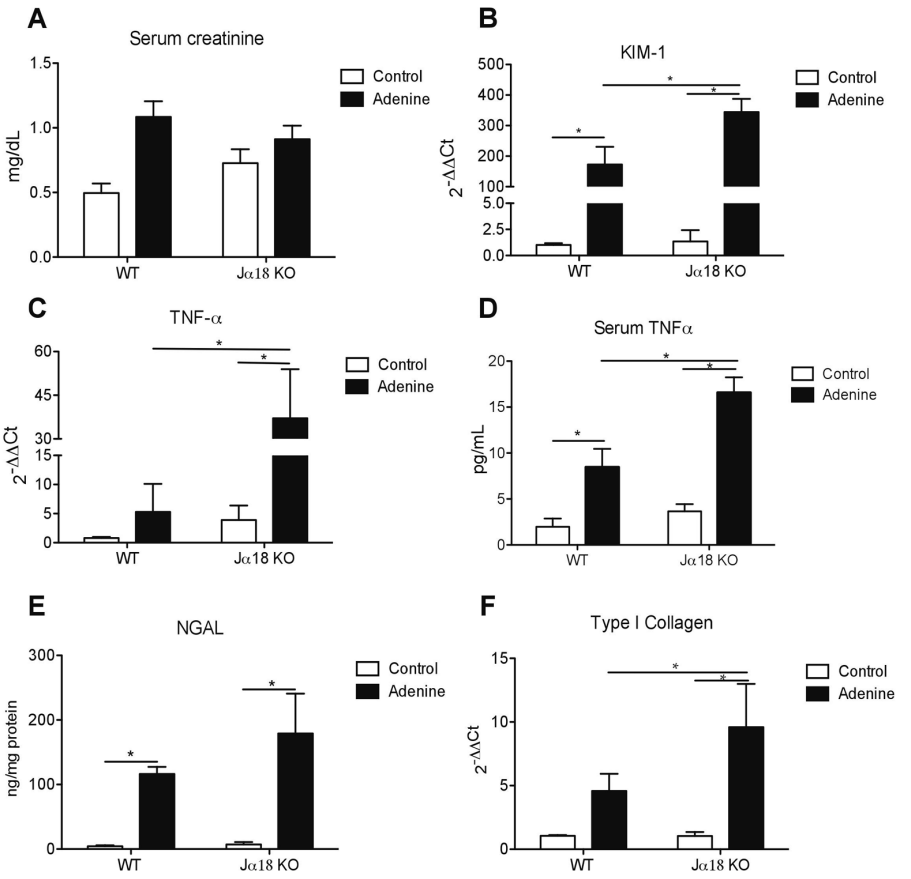

Figure 1. Analysis of renal injury parameters in adenine-fed WT and Jα18KO mice. (A) Renal function was assessed by serum creatinine levels from WT control, WT + adenine, Jα18KO control, and Jα18KO + adenine. n = 4–5 animals/group. Renal tissue from WT and Jα18KO mice was processed to determine: *KIM-1* mRNA expression (B), *TNF-α* mRNA expression (C), serum TNF-α levels (D), NGAL levels (E) and type I collagen mRNA expression (F). n = 3–5 animals/group. ANOVA, with Tukey posttest, *$p < 0.05$.

RESULTS

Adenine-Fed Jα18KO Mice Presented Higher Expression of *KIM-1*, *TNF-α* and Type I Collagen

To determine if the absence of iNKT cells would play a role in adenine-induced TIN, C57Bl/6J and Jα18KO mice were fed a 0.25% adenine diet for 10 d. Jα18KO mice lack iNKT cells. Compared to basal levels, serum creatinine levels increased in WT mice fed an adenine diet. Jα18KO mice presented an increment on serum creatinine, but it was not statistically different from basal levels (Figure 1A). Furthermore, we also analyzed kidney mRNA expression of some molecules related to kidney injury as *TNF-α* and *KIM-1*. We observed a significant increase in mRNA expression of *KIM-1* in Jα18KO mice that were fed the adenine diet compared with WT on the same adenine diet (Figure 1B). Furthermore, mRNA expression of *TNF-α* was also increased in adenine-fed Jα18KO mice compared with adenine-fed WT mice (Figure 1C). TNF-α was also measured in the serum, and the same pattern was observed (Figure 1D). Another parameter analyzed was NGAL. In our groups, NGAL was significantly increased in both adenine-fed WT and Jα18KO mice when compared with controls, but there was no differ-

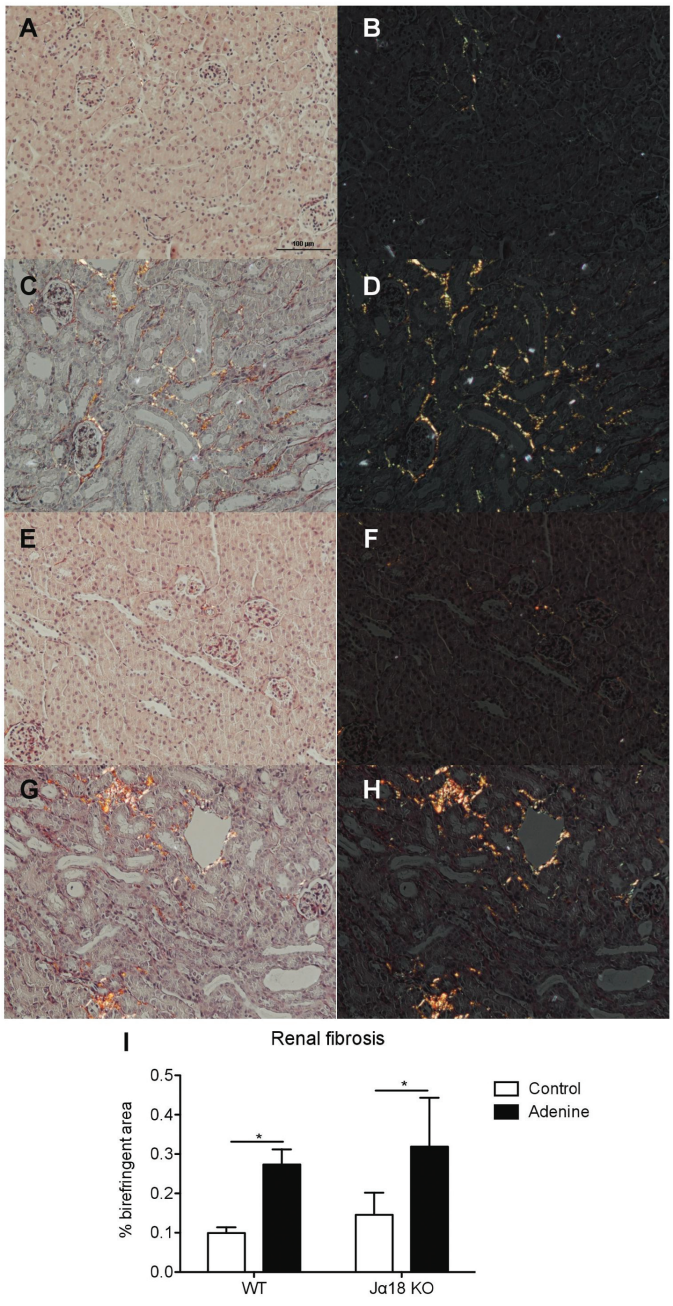

Figure 2. Quantification of renal fibrosis in adenine-fed WT and Jα18KO mice. Images are shown under common and polarized light in the panel. (A) WT control under common light. (B) WT control under polarized light. (C) WT + adenine under common light. (D) WT + adenine under polarized light. (E) Jα18KO control under common light. (F) Jα18KO control under polarized light. (G) Jα18KO + adenine under common light. (H) Jα18KO + adenine under polarized light. (I) Graphic quantification of collagen deposition by polarized light. ANOVA, with Tukey posttest, $^*p < 0.05$. n = 3–5 animals/group.

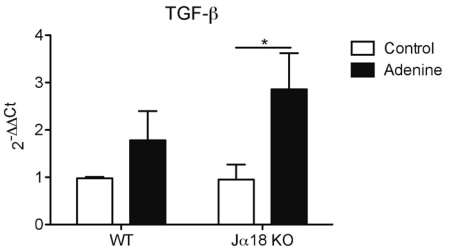

Figure 3. Analysis of *TGF-β* mRNA expression in renal tissue. Renal tissue from WT and Jα18KO mice were processed to determine mRNA expression of TGF-β. n = 3–4 animals/group. ANOVA, with Tukey posttest, $^*p < 0.05$.

ence between the adenine-fed groups (Figure 1E).

After insults and tissue injury, there is an attempt to heal the tissue with an increased production of extracellular matrix. If the insult persists, interstitial fibrosis may develop. Type I collagen is one of the components of extracellular matrix, and it is synthesized in response to injury (27); therefore, we analyzed mRNA expression of type I collagen (Figure 1F) and we performed the Sirius-red staining of the kidney tissue and analyzed it under polarized light to quantify the percentage of renal fibrosis (Figure 2). Type I collagen was significantly increased after adenine feeding in Jα18KO mice compared with Jα18KO control and to adenine-fed WT animals. Renal fibrosis was significantly increased after adenine ingestion in both WT and Jα18KO mice, and there was a tendency to higher fibrosis in adenine-fed Jα18KO mice. We also analyzed the histological changes after adenine feeding (Supplementary Figure S1) and observed that adenine-fed Jα18KO mice exhibited higher scores of tubular necrosis and tubular degeneration than adenine-fed WT mice. Also, transforming growth factor (TGF)-β is known to participate in the process of fibrogenesis, so we analyzed the mRNA expression of *TGF-β*, and we observed a significant increase only in adenine-fed Jα18KO mice compared with their controls (Figure 3).

To further investigate a role for iNKT cells in our renal injury model, we decided to activate them before tissue injury. This step could be relevant since other immune cells are involved in the process, and those cells could be masking the effect of iNKT cells deficiency.

Administration of αGalCer Reduced Creatinine Levels and Adenine-Induced Expression of *IL-6* and TNF-α in WT Mice at d 10

WT mice were injected once with 5 μg αGalCer (iNKT cells potent agonist) intraperitoneally on the same day they started receiving adenine diet (d 0). Animals were euthanized at d 4 and 10.

The 10th day is the late time point for this model, when we can detect the development of renal injury and fibrosis but not mortality. At this time point, serum creatinine was significantly reduced after αGalCer administration in adenine-fed WT mice (Figure 4A); however, NGAL levels (Figure 4B) were not. We also analyzed two proinflammatory cytokines, IL-6 and TNF-α. There was a significant reduction of *IL-6* mRNA expression (Figure 4C) in WT adenine-fed mice after αGalCer administration when compared with WT fed with adenine diet. mRNA expression of *TNF-α* had no difference between the groups (Figure 4D), but serum levels of TNF-α (Figure 4E) were significantly reduced after αGalCer administration in adenine-fed WT mice.

The activation of iNKT cells is a rapid process, and perhaps the late time point is showing only the final result of their activation early in the process; hence, we also analyzed some parameters in an early time point on the fourth day of adenine feeding. We analyzed serum creatinine levels and mRNA expression of *TNF-α*, *IL-6*, *IFN-γ*, signal transducer and activator of transcription-1 (*STAT-1*) and *IL-10*, and the results are shown in Figure 5. Although there was no difference in creatinine serum levels (Figure 5A) at d 4, the increased mRNA expression of *IL-6* (Figure 5B) and *TNF-α* (Figure 5C) in the adenine-fed groups shows that an inflammatory process may already be present in the kidney, and, at that time point, TNF-α is already decreasing in the group that received αGalCer. Concerning the other genes analyzed, we observed a significant increase in *IFN-γ* (Figure 5D), *STAT-1* (Figure 5E) and *IL-10* (Figure 5F) mRNA expression in the group that received αGalCer compared with control mice. We also observed, at this time point and not at d 10 (Figure 4F), a significant decrease in *TGF-β* mRNA expression (Figure 5G) in the group that received αGalCer compared with adenine-fed WT mice.

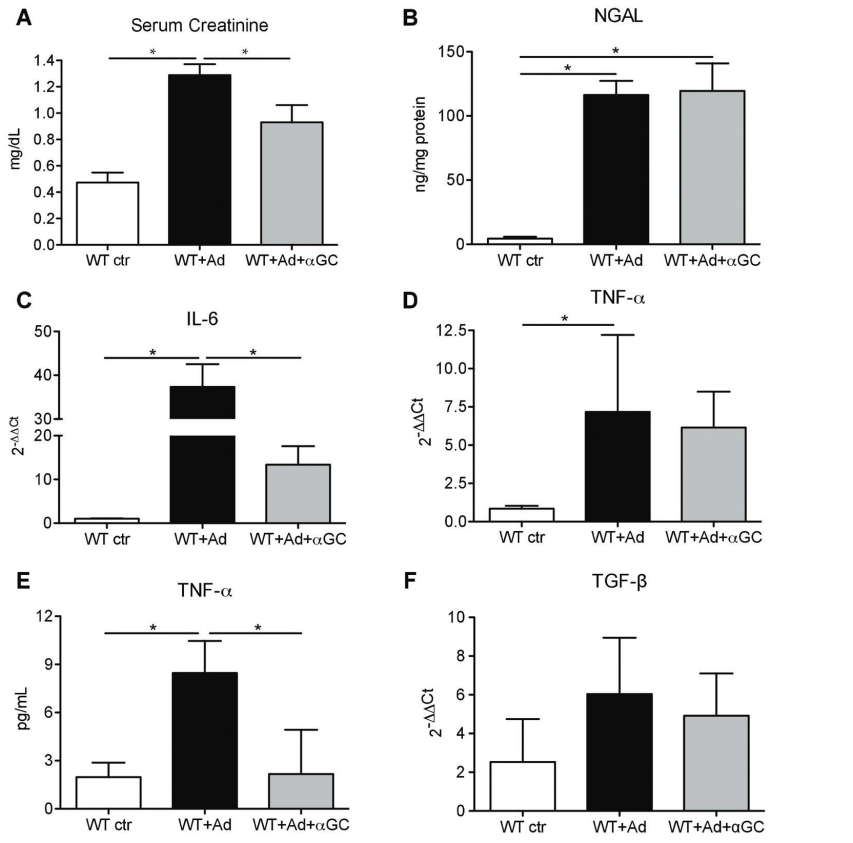

Figure 4. Administration of αGalCer improves renal function. Renal function was assessed at d 10 by serum creatinine levels (A) from WT control (ctr), WT + adenine (WT + Ad) and WT + adenine + αGalCer (WT + Ad + αGC). n = 5 animals/group. (B) NGAL levels were quantified in kidney extracts. mRNA expression of *IL-6* (C) and *TNF-α* (D) were quantified from kidney extracts. (E) TNF-α serum levels. (F) mRNA expression of *TGF-β* in the kidney. n = 3–5 animals/group. ANOVA, with Tukey posttest, $^*p < 0.05$.

αGalCer Challenge Reduced Renal Fibrosis and FSP-1 and α-SMA Staining in Renal Tissue

Because renal fibrosis is an important parameter of renal injury, we also quantified it using different methods. We analyzed renal tissue sections from the three groups (WT control, WT + adenine, and WT + αGalCer + adenine) at d 10. There was a significant decrease in renal fibrosis after αGalCer administration in adenine-fed WT mice compared with adenine-fed WT mice without αGalCer injection (Figure 6). To verify whether such reduction of renal fibrosis observed in our experiments was a consequence of a reduced number of fibroblasts and myofibroblasts, we analyzed immunohistochemistry staining for FSP-1 and α-SMA, respectively. According to our results, αGalCer challenge in adenine-fed WT mice was capable of decreasing both FSP-1 and α-SMA staining in renal tissue (Figures 7 and 8, respectively).

αGalCer Challenge Did Not Ameliorate Adenine-Induced Renal Injury in IFN-γKO Mice

It is still unclear how αGalCer attenuates the development of renal fibrosis.

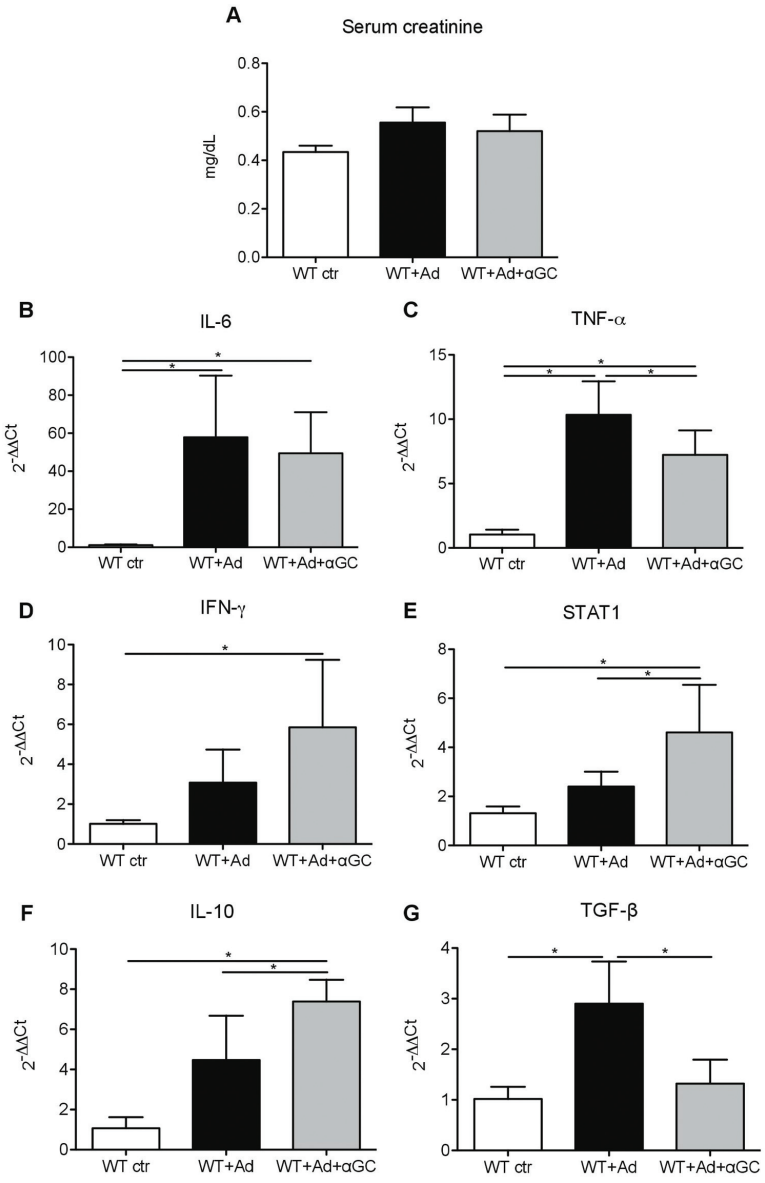

Figure 5. Analysis of serum creatinine and cytokine mRNA expression at d 4. (A) Serum levels of creatinine were assessed at d 4 of adenine feeding. mRNA expression of *IL-6* (B), *TNF-α* (C), *IFN-γ* (D), *STAT-1* (E) and *IL-10* (F) was also analyzed at d 4. n = 4–8 animals/group. ANOVA, with Tukey posttest, $*p < 0.05$.

However, among NKT cell–produced cytokines, IFN-γ is known to have antifibrotic effects in experimental models, including the bleomycin-induced pulmonary fibrosis model (28,29). Yet, as shown above, we observed an increase in *IFN-γ* and *STAT-1* (which is activated by IFN-γ and activates IFN-stimulated genes) gene expression after αGalCer administration.

To gain insight into the mechanism of protection conferred by αGalCer, we analyzed the role of IFN-γ in adenine-induced renal injury after αGalCer administration. Therefore, we submitted IFN-γKO mice to adenine feeding and also to αGalCer challenge.

Adenine ingestion was capable of inducing renal injury in IFN-γKO mice assessed by serum creatinine. However, αGalCer challenge could not improve renal function in these mice. We observed that there was no change in the parameters analyzed (serum creatinine; NGAL levels; *KIM-1*, *TNF-α* and *IL-6* mRNA expression; and renal fibrosis) (Figure 9) after αGalCer administration in adenine-fed IFN-γKO mice compared to adenine-fed IFN-γKO mice. Neither FSP-1 nor α-SMA staining was reduced after αGalCer challenge and adenine feeding (Supplementary Figure S2). Panels with representative images of renal fibrosis are shown in Supplementary Figure S3. These results may show that IFN-γ is an important factor in this model of renal injury, since αGalCer administration could not improve renal function in adenine-fed IFN-γKO mice.

DISCUSSION

The inflammatory process in kidney diseases is quite varied and involves the participation of cells, cytokines, chemokines and other factors. Several cell types participate in this process, with the contribution of T lymphocytes, neutrophils and macrophages. However, the role of NKT cells in renal diseases is still unclear. Our study demonstrated that αGalCer administration might improve renal function and injury in a model of adenine-induced tubule-interstitial nephritis.

The absence of NKT cells in KO mice had no significant influence on creatinine measurement, but led to a significant increase in gene expression of *KIM-1*, indicating that a deficiency in these cells may be detrimental to the kidney in this model. Another protein related to kidney injury is NGAL, and it was also increased after adenine feeding. These two tubular proteins might reflect a direct aggression of adenine crystals to renal tubules.

Since TNF-α is a proinflammatory cytokine and it is related to interstitial fibrosis, we also analyzed it. In our results, we observed a significant increase in gene expression of *TNF-α* and *TGF-β* in Jα18KO mice, indicating that the absence of invariant NKT cells may aggra-

vate the inflammatory process and consequently the renal interstitial fibrosis. Quantifying tubule-interstitial fibrosis and mRNA expression of type I collagen could best assess the involvement of these proinflammatory and profibrotic cytokines. mRNA expression of type I collagen was significantly increased in adenine-fed Jα18KO mice when compared with adenine-fed WT mice, which could indicate increased fibrosis. Renal fibrosis was increased in both WT and Jα18KO mice submitted to adenine feeding, but there was no difference between these two groups. Hence, we evaluated other histological changes besides fibrosis, and we analyzed tubular degeneration, tubular necrosis, inflammatory infiltrate and tubular hypertrophy. In two of these parameters, adenine-fed Jα18KO mice had higher scores, which could corroborate the other results suggesting that these KO mice present worse renal injury.

Because the inflammatory process in kidney diseases is complex and involves other immune cells, the absence of iNKT cells by themselves may not be the best method to assess their role. Thus, we also tested another technique to see how activated iNKT cells could participate in the injury process. To activate iNKT cells, we administered a known agonist of these cells, the glycolipid αGalCer. αGalCer is presented by antigen-presenting cells through the molecule CD1d. This complex binds to the TCR of NKT cells with high affinity, and such attachment activates iNKT cells (30,31). In our experiments, we observed that the administration of αGalCer could improve renal function in our model, since there was a decrease in serum creatinine levels, *IL-6* gene expression, serum TNF-α and renal fibrosis. Although NGAL levels were not reduced after αGalCer administration, this might imply that the tubular injury still exists because of the physical presence of crystals, but the inflammatory process could be minimized. A later time point analysis should be addressed in future studies to confirm this idea.

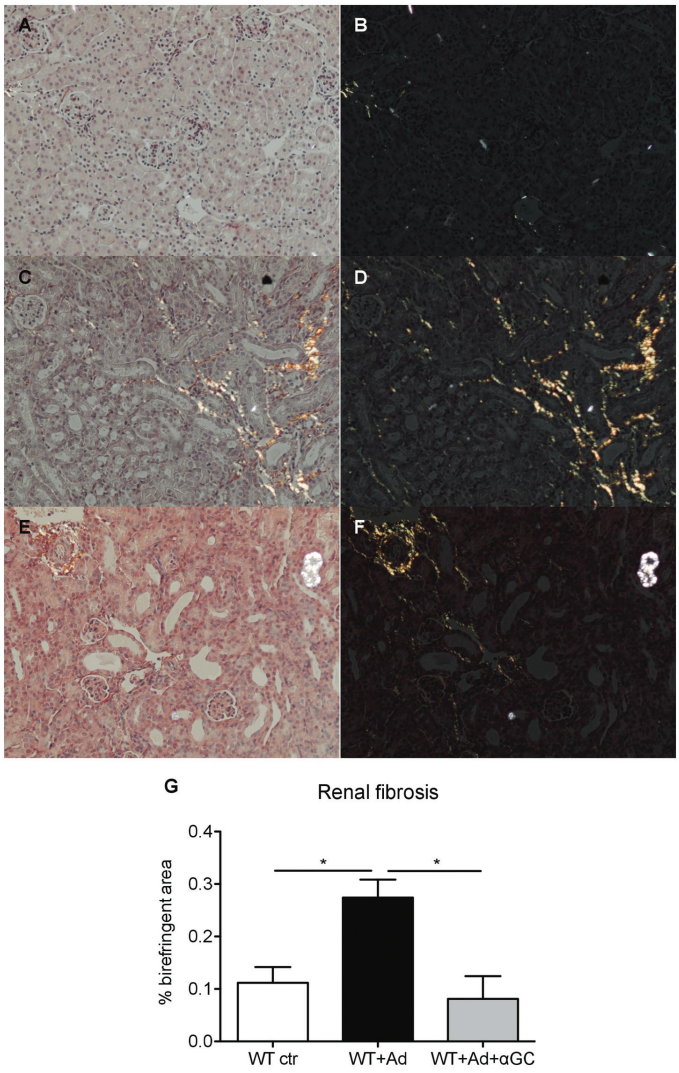

Figure 6. Reduction of renal fibrosis after αGalCer administration. Images of renal tissue: WT control (A), WT + adenine (C) and WT + adenine + αGalCer (E) under common light and WT control (B), WT + adenine (D) and WT + adenine + αGalCer (F) under polarized light. Graphic quantification of fibrosis deposition is shown in (G). n = 3–5 animals/group. ANOVA, with Tukey posttest, *$p < 0.05$.

Renal interstitial fibrosis is characterized by tubular atrophy, leukocyte infiltration, excessive deposition of extracellular matrix and accumulation of fibroblasts (24). Although other cells may be involved, the fibroblasts can be considered as key mediators of renal fibrosis (25,26), especially through the process of epithelial-mesenchymal transition. In this process, epithelial renal cells undergo transition to a fibroblast phenotype and contribute to the production of extracellular matrix components (4).

Given the important role of fibroblasts, we also analyzed in our study the FSP-1 expression in renal tissue. We observed that the administration of αGalCer in adenine-fed animals caused a significant reduction of FSP-1 and α-SMA compared with adenine-fed WT mice without αGalCer. Labeling of α-SMA is related to

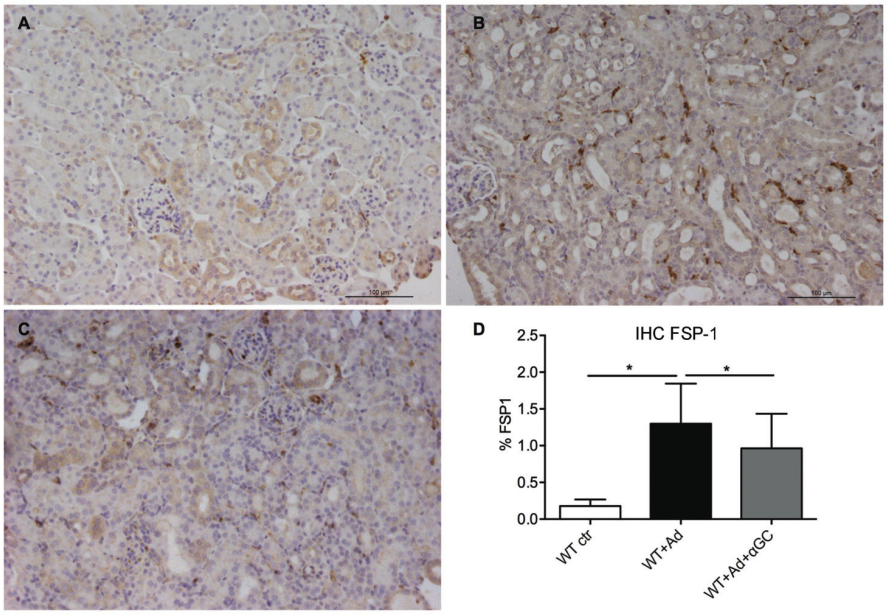

Figure 7. FSP-1 staining in renal tissue after αGalCer administration. Images of renal tissue after FSP-1 immunohistochemistry. (A) WT control. (B) WT + adenine. (C) WT + adenine + αGalCer. (D) Graphic quantification of positive staining. n = 3–5 animals/group. ANOVA, with Tukey posttest, *$p < 0.05$.

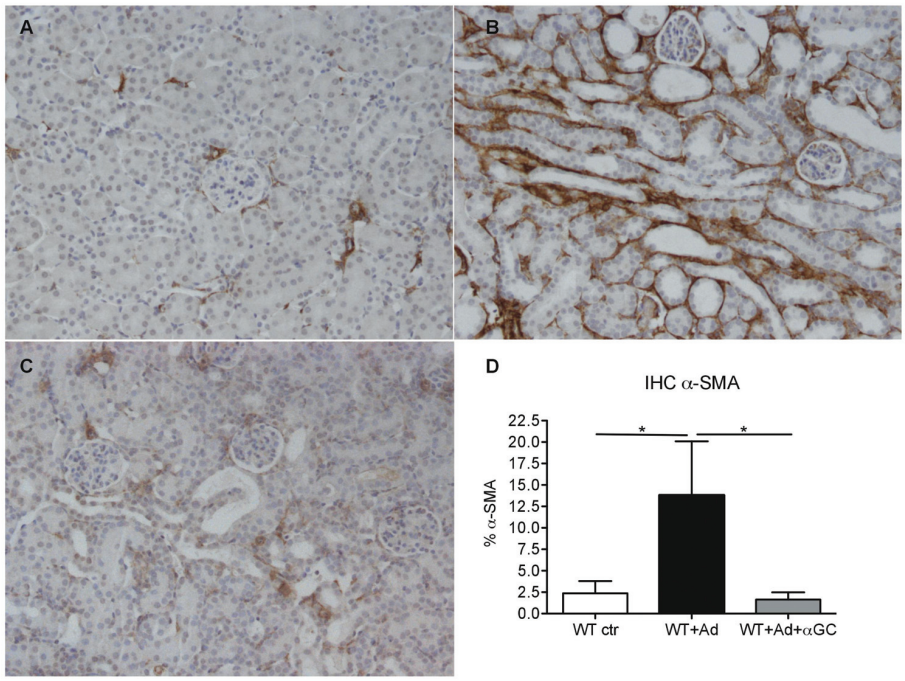

Figure 8. α-SMA staining in renal tissue after αGalCer administration. Images of renal tissue after α-SMA immunohistochemistry. (A) WT control. (B) WT + adenine. (C) WT + adenine + αGalCer. (D) Graphic quantification of positive staining. n = 3–5 animals/group. ANOVA, with Tukey posttest, *$p < 0.05$.

the contractile function acquired by the myofibroblasts during the fibrotic process. The acquisition of the myofibroblast phenotype may represent the response of the kidney fibroblasts to a stress that was recently proposed to be due to intratubular hydrodynamic forces and tubular stretch (for example, by obstruction, or in the case of our study, due to the deposition of adenine crystals within the tubules) (32).

The involvement of NKT cells in the process of fibrogenesis has been demonstrated in several studies with experimental models of liver, lung and kidney diseases. However, the role of NKT cells in some of these models is still controversial. In experimental models of liver diseases, Park *et al.* (33) demonstrated that carbon tetrachloride–induced liver injury led to increased hepatic fibrosis in Jα18KO mice. In experimental models of lung diseases, Kimura *et al.* (34) observed that the administration of αGalCer increased survival and reduced pulmonary fibrosis and TGF-β levels in the bleomycin model. In renal diseases, Pereira *et al.* (35) found that GSL-1 (another NKT agonist) modulates the development of experimental focal and segmental glomerulosclerosis (EFSG) and, in the study by Mesnard *et al.* (36), Jα18KO mice demonstrated worse renal function in anti–glomerular basement membrane (anti-GBM) glomerulonephritis. These data support our findings that Jα18 knockout mice are prone to a higher percentage of fibrosis and that administration of αGalCer was effective in reducing this process.

The study by Kimura *et al.* (34) also highlights an increase in IFN-γ levels after αGalCer treatment with a protective role in the bleomycin model. IFN-γ is the type II interferon synthesized by $CD4^+$ Th1 and $CD8^+$ lymphocytes, NK, B and NKT cells (37–41); it is considered to be a key player in Th1 immune responses with immunomodulatory effects on several immune cells (42), stimulating tumor cell cytotoxicity and antimicrobial activity and downregulating *TGF-β* and type I and II procolla-

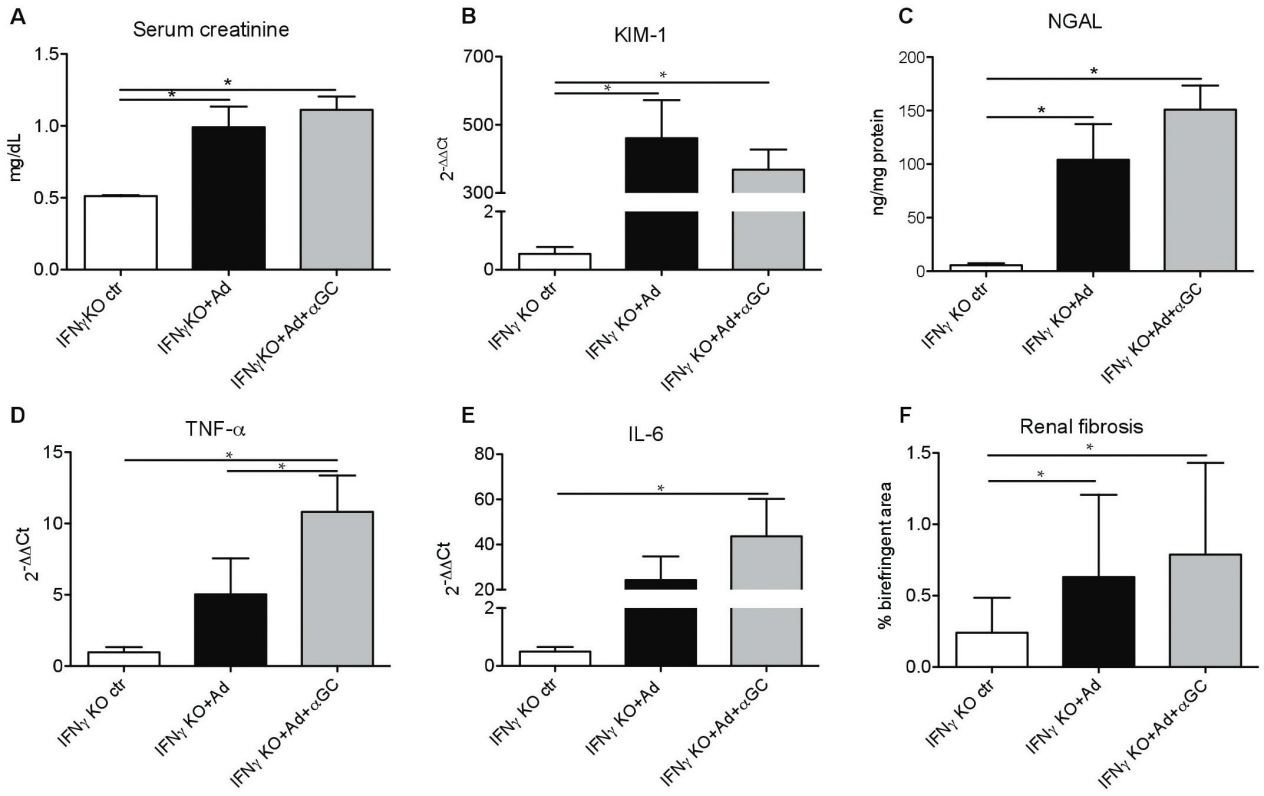

Figure 9. Renal function in IFN-γKO mice after adenine feeding. Renal function was assessed by serum creatinine levels (A), mRNA expression of *KIM-1* (B), NGAL levels (C), mRNA expression of *TNF-α* (D), mRNA expression of *IL-6* (E) and graphic quantification of fibrosis deposition (F), from IFN-γKO control, IFN-γKO + adenine and IFN-γKO + adenine + αGalCer. n = 3–5 animals/group. ANOVA, with Tukey posttest, $*p < 0.05$.

gens gene expression in lung fibrosis models (28,43). In renal diseases models, Kimura *et al.* (44) reported a protective role of IFN-γ in cisplatin-induced renal injury. In this case, IFN-γ can accelerate autophagic flux and therefore increase the viability of renal tubular cells. In our study, we observed increased mRNA expression of *IFN-γ* and *STAT-1* at d 4 in mice receiving αGalCer and adenine diet. We also used IFN-γKO mice to observe its contribution in the adenine-induced renal injury model. The excessive ingestion of adenine in IFN-γKO mice also caused renal injury, but it was not improved after αGalCer administration, as we observed in WT mice. Our findings may indicate that the release of IFN-γ is one of the main factors contributing to the improvement in renal function after αGalCer administration. The pathways by which IFN-γ mediates the improvement observed in our study must be analyzed in further studies.

Taken together, previous studies and ours show that NKT cells may have different functions depending on the organ and/or the stimuli of the microenvironment in which they are set. However, their participation in the process of fibrogenesis and the mechanisms involved in it are not fully understood, which demonstrates the contribution of our work in attempting to elucidate the plasticity of these cells and their mechanisms of action in diseases.

ACKNOWLEDGMENTS

The authors thank Masaru Taniguchi at the RIKEN Research Center for Allergy and Immunology (Japan) for Jα18KO mice and Paulo Albe for preparing the histology slides. This work was supported by Coordenação de Aperfeiçoamento de Pessoal de Nível Superior (CAPES), Fundação de Amparo à Pesquisa do Estado de São Paulo (FAPESP grant numbers 07/07139-3, 2012/02270-2 and 2012/16794-3) and Conselho Nacional de Desenvolvimento Científico e Tecnológico (CNPq, Complex Fluids INCT). The funders had no role in study design, data collection and analysis; decision to publish; or preparation of the manuscript.

DISCLOSURE

The authors declare that they have no competing interests as defined by *Molecular Medicine*, or other interests that might be perceived to influence the results and discussion reported in this paper.

REFERENCES

1. Stevens LA, Coresh J, Greene T, Levey AS. (2006) Assessing kidney function: measured and estimated glomerular filtration rate. *N. Engl. J. Med.* 354:2473–83.
2. Stockelman MG, *et al.* (1998) Chronic renal failure in a mouse model of human adenine phosphoribosyltransferase deficiency. *Am. J. Physiol.* 275:F154–63.
3. Thadhani R, Pascual M, Bonventre JV. (1996) Acute renal failure. *N. Engl. J. Med.* 334:1448–60.
4. Iwano M, *et al.* (2002) Evidence that fibroblasts derive from epithelium during tissue fibrosis. *J. Clin. Invest.* 110:341–50.
5. Liu Y. (2010) New insights into epithelial-mesenchymal transition in kidney fibrosis. *J. Am. Soc. Nephrol.* 21:212–22.
6. Yokozawa T, Oura H, Koizumi F. (1985) 2,8-Dihydroxyadenine urolithiasis induced by dietary adenine in rats. *Nihon Jinzo Gakkai shi.* 27:371–8.
7. Engle SJ, *et al.* (1996) Adenine phosphoribosyltransferase-deficient mice develop 2,8-dihydroxyadenine nephrolithiasis. *Proc. Nalt. Acad. Sci. U. S. A.* 93:5307–12.
8. Correa-Costa M, *et al.* (2011) Pivotal role of Toll-like receptors 2 and 4, its adaptor molecule MyD88, and inflammasome complex in experimental tubule-interstitial nephritis. *PLoS One.* 6:e29004.
9. Okabe C, *et al.* (2013) NF-kappaB activation mediates crystal translocation and interstitial inflammation in adenine overload nephropathy. *Am. J. Physiol. Renal Physiol.* 305:F155–63.
10. Kronenberg M. (2005) Toward an understanding of NKT cell biology: progress and paradoxes. *Ann. Rev. Immunol.* 23:877–900.
11. Chiu YH, *et al.* (1999) Distinct subsets of CD1d-restricted T cells recognize self-antigens loaded in different cellular compartments. *J. Exp. Med.* 189:103–110.
12. Arrenberg P, Halder R, Kumar V. (2009) Cross-regulation between distinct natural killer T cell subsets influences immune response to self and foreign antigens. *J. Cell. Physiol.* 218:246–50.
13. Bendelac A, Savage PB, Teyton L. (2007) The biology of NKT cells. *Ann. Rev. Immunol.* 25:297–336.
14. Van Kaer L. (2005) Alpha-galactosylceramide therapy for autoimmune diseases: prospects and obstacles. *Nat. Rev. Immunol.* 5:31–42.
15. Yoshimoto T, Paul WE. (1994) CD4pos, NK1.1pos T cells promptly produce interleukin 4 in response to in vivo challenge with anti-CD3. *J. Exp. Med.* 179:1285–95.
16. Baccala R, Kono DH, Theofilopoulos AN. (2005) Interferons as pathogenic effectors in autoimmunity. *Immunol. Rev.* 204:9–26.
17. Cui J, *et al.* (1997) Requirement for Valpha14 NKT cells in IL-12-mediated rejection of tumors. *Science.* 278:1623–6.
18. Kjeldsen L, Cowland JB, Borregaard N. (2000) Human neutrophil gelatinase-associated lipocalin and homologous proteins in rat and mouse. *Biochim. Biophys. Acta.* 1482:272–83.
19. Hraba-Renevey S, Turler H, Kress M, Salomon C, Weil R. (1989) SV40-induced expression of mouse gene 24p3 involves a post-transcriptional mechanism. *Oncogene.* 4:601–8.
20. Mishra J, *et al.* (2003) Identification of neutrophil gelatinase-associated lipocalin as a novel early urinary biomarker for ischemic renal injury. *J. Am. Soc. Nephrol.* 14:2534–43.
21. Mishra J, *et al.* (2004) Neutrophil gelatinase-associated lipocalin: a novel early urinary biomarker for cisplatin nephrotoxicity. *Am. J. Nephrol.* 24:307–15.
22. Han WK, Bailly V, Abichandani R, Thadhani R, Bonventre JV. (2002) Kidney Injury Molecule-1 (KIM-1): a novel biomarker for human renal proximal tubule injury. *Kidney Int.* 62:237–44.
23. Ramesh G, Reeves WB. (2005) p38 MAP kinase inhibition ameliorates cisplatin nephrotoxicity in mice. *Am. J. Physiol. Renal Physiol.* 289:F166–74.
24. Zeisberg M, Strutz F, Muller GA. (2001) Renal fibrosis: an update. *Curr. Opin. Nephrol. Hypertens.* 10:315–20.
25. Strutz F, Zeisberg M. (2006) Renal fibroblasts and myofibroblasts in chronic kidney disease. *J. Am. Soc. Nephrol.* 17:2992–8.
26. Eddy AA, Neilson EG. (2006) Chronic kidney disease progression. *J. Am. Soc. Nephrol.* 17:2964–6.
27. Kadler KE, Holmes DF, Trotter JA, Chapman JA. (1996) Collagen fibril formation. *Biochem. J.* 316:1–11.
28. Gurujeyalakshmi G, Giri SN. (1995) Molecular mechanisms of antifibrotic effect of interferon gamma in bleomycin-mouse model of lung fibrosis: downregulation of TGF-beta and procollagen I and III gene expression. *Exp. Lung Res.* 21:791–808.
29. Hyde DM, Henderson TS, Giri SN, Tyler NK, Stovall MY. (1988) Effect of murine gamma interferon on the cellular responses to bleomycin in mice. *Exp. Lung Res.* 14:687–704.
30. Roark JH, *et al.* (1998) CD1.1 expression by mouse antigen-presenting cells and marginal zone B cells. *J. Immunol.* 160:3121–7.
31. Brossay L, *et al.* (1997) Mouse CD1 is mainly expressed on hemopoietic-derived cells. *J. Immunol.* 159:1216–24.
32. Boor P, Ostendorf T, Floege J. Renal fibrosis: novel insights into mechanisms and therapeutic targets. *Nat. Rev. Nephrol.* 6:643–56.
33. Park O, *et al.* (2009) Diverse roles of invariant natural killer T cells in liver injury and fibrosis induced by carbon tetrachloride. *Hepatology.* 49:1683–94.
34. Kimura T, *et al.* (2004) Treatment with alpha-galactosylceramide attenuates the development of bleomycin-induced pulmonary fibrosis. *J. Immunol.* 172:5782–9.
35. Pereira RL, *et al.* (2012) Invariant natural killer T cell agonist modulates experimental focal and segmental glomerulosclerosis. *PLoS One.* 7:e32454.
36. Mesnard L, *et al.* (2009) Invariant natural killer T cells and TGF-beta attenuate anti-GBM glomerulonephritis. *J. Am. Soc. Nephrol.* 20:1282–92.
37. Frucht DM, *et al.* (2001) IFN-gamma production by antigen-presenting cells: mechanisms emerge. *Trends Immunol.* 22:556–60.
38. Flaishon L, *et al.* (2000) Autocrine secretion of interferon gamma negatively regulates homing of immature B cells. *J. Exp. Med.* 192:1381–8.
39. Harris DP, *et al.* (2000) Reciprocal regulation of polarized cytokine production by effector B and T cells. *Nat. Immunol.* 1:475–82.
40. Baker J, Verneris MR, Ito M, Shizuru JA, Negrin RS. (2001) Expansion of cytolytic CD8(+) natural killer T cells with limited capacity for graft-versus-host disease induction due to interferon gamma production. *Blood.* 97:2923–31.
41. Asai O, *et al.* (1998) Suppression of graft-versus-host disease and amplification of graft-versus-tumor effects by activated natural killer cells after allogeneic bone marrow transplantation. *J. Clin. Invest.* 101:1835–42.
42. Knothe S, *et al.* (2011) The NKT cell ligand alpha-galactosylceramide suppresses allergic airway inflammation by induction of a Th1 response. *Vaccine.* 29:4249–55.
43. Abbas AK, Murphy KM, Sher A. (1996) Functional diversity of helper T lymphocytes. *Nature.* 383:787–93.
44. Kimura A, *et al.* (2012) Interferon-gamma is protective in cisplatin-induced renal injury by enhancing autophagic flux. *Kidney Int.* 2:1093–104.

Cite this article as: Aguiar CF, *et al.* (2015) Administration of α-galactosylceramide improves adenine-induced renal injury. *Mol. Med.* 21:553–62.